NASA TECHNICAL NOTE

NASA TN D-2004

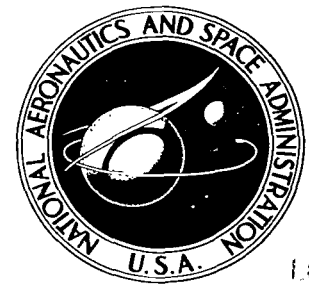

THREE-BODY COLLISIONAL RECOMBINATION OF CESIUM SEED IONS AND ELECTRONS IN HIGH-DENSITY PLASMAS WITH ARGON CARRIER GAS

by John V. Dugan, Jr.

Lewis Research Center
Cleveland, Ohio

NATIONAL AERONAUTICS AND SPACE ADMINISTRATION • WASHINGTON, D. C. • OCTOBER 1964

THREE-BODY COLLISIONAL RECOMBINATION OF CESIUM SEED IONS AND ELECTRONS IN HIGH-DENSITY PLASMAS WITH ARGON CARRIER GAS

By John V. Dugan, Jr.

Lewis Research Center
Cleveland, Ohio

NATIONAL AERONAUTICS AND SPACE ADMINISTRATION

For sale by the Office of Technical Services, Department of Commerce,
Washington, D.C. 20230 -- Price $1.00

THREE-BODY COLLISIONAL RECOMBINATION OF CESIUM SEED IONS AND ELECTRONS IN HIGH-DENSITY PLASMAS WITH ARGON CARRIER GAS*

by John V. Dugan, Jr.

Lewis Research Center

SUMMARY

The rate of three-body recombination between cesium seed ions and electrons in an argon carrier gas is calculated for free-electron number densities of 10^{13} to 10^{18} per cubic centimeter and electron temperatures of 500° to $10,000^{\circ}$ K. These ranges correspond to plasmas of interest for magnetohydrodynamic power generation. Only monatomic cesium ions are considered in a collisional approximation where radiative transitions are ignored. The Byron method is applied to describe collision-induced transitions between atomic energy levels by the semiclassical Gryzinski cross sections and the principle of detailed balancing. Recombination is limited by deexcitation due to superelastic collisions.

Results are in fair agreement with those of a more approximate study of potassium for 500° to 2000° K. Discussion of the results as related to conductivity in magnetohydrodynamic power generation and comparison with recombination experiments are included. The computer program for a general recombination study of an atomic ion is included as an appendix.

INTRODUCTION

Recombination Problem in the Magnetohydrodynamic Generator

The requirements of magnetohydrodynamic (MHD) power generation set lower limits on allowable conductivity values for gas dynamic systems employing alkali-seeded rare gases. The electrical conductivity in the generator duct is a function of the free-electron number density N_e, which must be maintained by electron-atom ionizing collisions. However, if the electrons initially produced by ionizing collisions recombine with positive ions in a time that is

*A brief summary of some of the results presented in this report was given at the American Physical Society Meeting, Plasma Physics Section, San Diego, Calif., Nov. 2-6, 1963.

short compared with a characteristic ionization time, volume recombination will severely inhibit attainment of the conductivity values required for efficient generator operation. A recent paper predicts high recombination rates for a potassium ion plasma over all number densities in an electron temperature range from 500° to 2000° K (ref. 1). The object of the present report is to estimate the net rate of electron-ion recombination in a plasma of argon (ionization potential, 15.76 ev) seeded with varying percentages of cesium vapor (ionization potential, 3.89 ev). These gases have been considered a promising carrier-seed combination for magnetohydrodynamic power generation; consequently, the system has been the subject of extensive study (refs. 2 and 3).

Selection of Electron Capture Mechanism

It is well documented that three-body capture

$$Cs^{+} + e^{-} + e^{-} \rightarrow Cs^{*} + e^{-} \text{ (K.E.)}$$

is the initial step of the neutralization process in the plasmas of interest (refs. 1 to 4); Cs^{*} represents an excited or ground-state seed atom. This capture step is a radiationless process where the second electron carries away the excess energy as kinetic energy. D'Angelo performed a calculation on a fully ionized gas composed only of protons and electrons (ref. 4). He postulated the aforementioned three-body initial capture step and predicted recombination rates in agreement with several sets of experimental data, but his model has since proven inadequate for dense plasmas ($N_e > 10^{12}$ cm^{-3}) because he ignored deexcitation collisions (ref. 5). Bates, et al. (ref. 2) and the investigators of references 1 and 3 have performed more general studies in which they have included this effect.

It was proposed in reference 6 that the neutral carrier atom is the third body for certain cesium seeded systems. This cannot be the case for the seeded argon system because of efficiency requirements for energy transfer in the three-body encounter. The electron, on the average, can transfer only the fraction $2m_e/M$ of its translational energy to a neutral argon atom in an elastic collision where m_e and M are the electron and neutral masses, respectively. Since the first excited state of argon lies 11 electron volts above the electronic ground state, only very few electrons could transfer energy inelastically to the atomic third body for the θ_e values of interest. As a result, only electrons in the extreme low-energy portion of the Maxwellian distribution can successfully engage in a one-act capture process where an atom serves as the third body. On the other hand, electrons can exchange any amount of kinetic energy in their collisions with one another and thus would be the most effective third bodies for recombination.

Byron Approach

Once electrons are captured into excited states of the atom, they are not considered to have recombined effectively with the ion since they may have a high probability of being reionized. Byron, et al. (refs. 1 and 3) have shown

that the rate-limiting step in the "chain" of three-body-recombination processes is the deexcitation of captured electrons. Their model utilizes the rate-process principle that the slowest step in a rate mechanism is the limiting step. As the system approaches equilibrium, the rate at which electronic levels are crossed in the downward direction toward the ground state determines the net recombination rate. This is true because once the electron has reached the ground state it has a much smaller probability of being reionized than it had in the higher states.

The authors of reference 3 have shown that there is a minimum in the electronic deexcitation rate at a particular atomic energy level. The location of this level depends strongly on the temperature of the free electron gas.

In their application of the rate-limiting model to potassium ion-electron recombination, Byron, et al. assumed that the electronic levels above and below a quantum state L^* are continuous bands of energy levels rather than discrete states. They did not list the states included in their study nor the degeneracies assigned to those states. In addition, they approximated the slope of the Gryzinski cross section by a linear function in the electron temperature range, 500° to 2000° K, over which the calculation was performed.

The present report uses the same cross section expressions, in an exact fashion, with the rate-limiting model just described, and applies the method to cesium recombination. It proposes to assess the accuracy of the approximations given in reference 3 and extends the range of the recombination coefficients to temperatures from 2000° to $10{,}000^\circ$ K. Any quantum effects obscured by the continuum approximation of Byron, et al. should appear in this more exact study. Further, the information contained herein is designed to provide a basis for calculating recombination in high-pressure plasmas in addition to assessing the assumptions of the Maxwellian distribution function and the neglect of radiation.

The computer program for treating this three-body recombination of any monatomic species is described in appendix D by L. U. Albers. This program is included so that investigators can readily perform machine calculations on systems of interest.

PRESENT STUDY

Scope

The recombination model adopted herein is applied to calculating net recombination rates for electron number densities N_e from 10^{13} to 10^{18} particles per cubic centimeter and electron temperatures θ_e from 500° to $10{,}000^\circ$ K for a conventional range of cesium seed fractions from 5×10^{-4} to 10^{-2}. (All symbols are defined in appendix A.) These are the ranges of interest for magnetohydrodynamic generators. Number densities below 10^{13} per cubic centimeter will not provide sufficient conductivity for generator operation, while number densities of ionized seed N_+ (where $N_+ = N_e$) greater than 10^{18} per cubic centimeter correspond to neutral-carrier-gas densities of at least 10^{20}

region, N_e greater than 10^{18} per cubic centimeter, significant overlap of capture orbitals for electrons may preclude employment of the adopted recombination model, since collective interactions become important. With regard to electron temperatures, it appears that the most promising systems may make use of the high nonequilibrium θ_e values from 2000° to 8000° K (ref. 7); however, the electrons must be "Joule heated" from the static gas temperature, and this necessitates a recombination study at θ_e values down to 500° K. This temperature is a safe lower limit, since the coldest electrons will be at least in thermal equilibrium with gas atoms.

Collisional Approximation

It is assumed that all deexcitation is collisional so that all radiative deexcitations can be neglected. The validity of this assumption is discussed in appendix B, which indicates that radiation from excited seed atoms is negligible down to N_e values of about 10^{14} per cubic centimeter for all electron temperatures. Two-body electron-ion radiative recombination is also negligible in the N_e range considered. Further, it is assumed that the sole ionic species of importance is the cesium atomic ion; that is, the relative abundances of argon-cesium ions ($ArCs^+$) and argon ions are very small compared with the cesium ion concentration. This is a good approximation, since the argon-cesium ion ($ArCs^+$) is bound by weak polarization energy of less than thermal energy even at the lowest temperatures, while ionization of argon will have a relatively long relaxation time compared with cesium ionization (ref. 8). Thus, argon can effectively be neglected; preliminary calculations indicate that this is a good approximation to seed fractions of 2×10^{-4} for temperatures below 8500° K. At higher electron temperatures there may be some ionization of argon, at least near the entrance region of the generator duct for representative gas residence times (ref. 9).

Distribution Function Considerations

Throughout this study, it is assumed that a Maxwellian distribution of free electrons is preserved in the plasma. This is a reasonable assumption for the argon-cesium seed system, as can be shown from collision-frequency considerations. The electron-electron monoenergetic collision cross section for momentum transfer at these low energies (<1 ev) is relatively high, as seen even for the hard-sphere low estimate, which can be written as $Q_{ee} \cong 656/w^2$ angstrom^2 (ref. 10). The quantity w is the kinetic energy of the electron in electron volts. The related collision frequency is given by $\nu_{ee} = N_e Q_{ee} v_e$, where v_e is the relative velocity of the electrons. The frequency of electron-neutral encounters is given by $\nu_{en} = N_n Q_{en} v_{en}$, where N_n is the neutral argon number density, Q_{en} is the elastic electron-neutral collision cross section, and v_{en} is the electron-neutral relative velocity. Even though N_e is less than or equal to $10^{-2}\ N_n$ for the plasmas of interest, the ν_{ee} value will nevertheless be greater than ν_{en}, because, due to the Ramsauer effect (ref. 11), the argon atoms are virtually transparent to electrons in the range of energy from 0.1 to 1.0 electron volt, so that the average Q_{en} is

only 3 angstroms^2. This value is the average value of Q_{en} from 0.1 to 1.0 electron volt for Maxwellian distributions of electrons at each electron temperature. Elastic collisions between electrons and seed atoms are assumed to have maximum cross sections of the order of the Q_{ee} value. This latter assumption is well founded since the (pessimistic) minimum Q_{ee} (at 1 ev) is 656 angstroms^2, while the maximum calculated Q_{en} for cesium neutrals is 600 angstroms^2 (averaged over the Maxwellian distribution at 0.5 ev, ref. 12). Consequently, the electron collision frequency is certainly greater than either electron-neutral (carrier or seed) collision frequency. The assumption of a Maxwellian electron distribution should therefore be valid.

DETAILS OF CALCULATION

The deexcitation rate R_{dex} is defined herein as the rate at which electrons in discrete energy states K above a state L^* can pass downward either to L^* or past that state to all states L below it, across the energy gap $K^* \rightarrow L^*$, where $K^* = L^* + 1$. It is assumed that all the electronic states are in equilibrium with the free electrons at the electron temperature. This is not quite true for the lower states, whose populations are less than the equilibrium values because they require a longer time to attain equilibrium populations. To account for these and other nonequilibrium effects, a temperature-dependent factor γ is introduced to relate the minimum deexcitation rate to the recombination rate.

For a hypothetical nonequilibrium situation (1) with no reexcitation occurring during the period of deexcitation and (2) state populations above the limiting gap equal to equilibrium values, γ would be unity, and the net recombination rate would be equal to the deexcitation rate for the slowest or rate-determining transition. Clearly, at equilibrium where $R_{dex} = R_{ex}$ across all gaps, there is no net recombination and γ must be zero. The calculation of recombination rate, therefore, consists of determining the minimum deexcitation rate and the value of γ for the range of electron temperatures and densities of interest.

Collision Cross Sections and Deexcitation

For a one-electron outer shell, such as that of the singly excited or ground state cesium atom, the ionization potential (or binding energy) is equal to the kinetic energy of the bound electron. Gryzinski (ref. 13) has derived cross section expressions for the inelastic collision of an electron with an atom by treating such a collision as a classical encounter between the free electron and the bound electron. Although these expressions predict a low value and the wrong energy dependence of the ionization cross section at the threshold ($\propto E^{1/2}$ instead of the experimentally observed $\propto E$ (ref. 14)), they should be satisfactory for calculating the recombination rate within a factor of two to four (ref. 15). Experimental error in recombination-rate measurements is somewhat less (refs. 5 and 16), so that discrepancies between predicted and observed rates can be explained, at least, in part, as due to inadequate cross sections.

The main deexcitation route in the range of interest for N_e and θ_e is through superelastic collisions whereby the incident (free) electron receives the energy of atomic deexcitation from the bound electron as increased kinetic energy (refs. 1, 2, and 16).

In the Byron approach, the deexcitation rate is not computed directly through the deexcitation cross section but must be obtained from the excitation rate by using the statistical mechanical principle of detailed balancing (ref. 17). The inelastic excitation cross section necessary to calculate the excitation rate is discussed in the following section. The Gryzinski expressions have been remarkably successful (in view of their derivation on a purely semiclassical basis) in predicting collisional excitation probabilities from ground to lower excited states for some atoms.

Energy Levels of Cesium Atom Quantum Degeneracy

The first 70 observed spectral levels of the cesium atom selected for the calculation are taken from reference 18. Because of pressure and Doppler broadening (ref. 1) and external magnetic-field effects (B may be as high as 20,000 gauss), it was thought reasonable to assume that energy states separated by 30 wave numbers or less are effectively degenerate in energy. The 47 electronic "uncollapsed" states are listed in table I with their binding energies E_1. The n and l values are the principal and secondary (orbital) quantum numbers, whereas $S_p = 1/2$ is the spin of one unpaired electron in units of $\hbar$.

The total degeneracy of an electronic energy level ω is given. Spin-orbit coupling removes the spin degeneracy, giving rise to the spin-orbit quantum number $J = l \pm S_p$.

Eighteen of the listed levels are nondegenerate in J value. The remaining 29 levels denoted by asterisks are degenerate levels. Seven of these states degenerate in J are s states ($l = 0$) where the spin degeneracy can only be removed in an external magnetic field. The other 22 states are p, d, f, g, and h states ($l = 1$ to 5) where l-s coupling is not strong enough to split the levels by more than 30 wave numbers (cm^{-1}) in energy.

Excitation Cross Section

The cross section (cm^2) for inelastic collision between an incident electron with energy E_2 and an atomic electron with kinetic energy (or binding energy) E_1 occurring with an energy loss greater than ΔE is (ref. 13)

$$Q_{ex}(E_2,E_1,\Delta E) = \frac{\sigma_0}{\Delta E^2}\left(\frac{E_2}{E_1 + E_2}\right)^{3/2}\left\{\frac{2}{3}\left[\left(\frac{E_1}{E_2}\right) + \frac{\Delta E}{E_2}\left(1 - \frac{E_1}{E_2}\right) - \left(\frac{\Delta E}{E_2}\right)^2\right]\right\} \quad (1a)$$

for $\Delta E + E_1 \leq E_2$

and

$$Q_{ex}(E_2,E_1,\Delta E) = \frac{\sigma_0}{\Delta E^2}\left(\frac{E_2}{E_1+E_2}\right)^{3/2}\left\{\frac{2}{3}\left[\left(\frac{E_1}{E_2}\right)+\frac{\Delta E}{E_2}\left(1-\frac{E_1}{E_2}\right)-\left(\frac{\Delta E}{E_2}\right)^2\right]\right.$$

$$\left.\times\left[\left(1+\frac{\Delta E}{E_1}\right)\left(1-\frac{\Delta E}{E_2}\right)\right]^{1/2}\right\} \qquad (1b)$$

$$\text{for} \quad \Delta E + E_1 \geq E_2$$

In both expressions

$$\sigma_0 = \pi e^4\left(\frac{ev}{erg}\right)^2 \text{ cm}^2 \text{ erg}^2$$

$$= \pi\,\frac{(4.8\times10^{-10})^4}{(1.6\times10^{-12})^2}$$

$$= 6.53\times10^{-14} \text{ (cm}^2\text{)(ev}^2\text{)}$$

where e is the electronic charge.

The mean product of cross section and velocity (cm^3/sec), integrated over the Maxwellian distribution, for the excitation of an electron from an energy level L up to an energy level K is (ref. 19, pp. 677-699)

$$\langle vQ_{ex}(L\rightarrow K)\rangle = \frac{8\pi\sigma_0}{C_0}\left[\frac{1}{\Delta E_{L,K}^2}\int_{\Delta E_{L,K}}^{\infty} G(E_2,E_1,\Delta E_{L,K})\right.$$

$$\left.-\frac{1}{\Delta E_{L,K+1}^2}\int_{\Delta E_{L,K+1}}^{\infty} G(E_2,E_1,\Delta E_{L,K+1})\right]F(E_1,E_2)E_2\,dE_2 \qquad (2)$$

where $G(E_2,E_1,\Delta E)$ is the function in braces of equation (1a) or (1b), $F(E_1,E_2) = \left[E_2/(E_1+E_2)\right]^{3/2} e^{-E_2/k\theta_e}$, and C_0 is the normalization factor for the Maxwellian distribution function, $(2\pi k\theta_e)^{3/2}(m_e)^{1/2}$.

An electron that is excited above the level K, ($\Delta E > \Delta E_{L,K}$), but not as high as the level K + 1, ($\Delta E < \Delta E_{L,K+1}$), can reach the level K by emitting radiation. This is a physical basis for the two lower limits in the integral expression for the mean excitation cross section.

The appropriate Q_{ex} should be employed for the two sets of conditions mentioned in equations (1a) and (1b).

Excitation Rate and Detailed Balancing

The corresponding rate at which electrons can be excited from the state L to state K is

$$r_{ex} = N_e N_L \langle (Q_{L,K})v \rangle \qquad \text{cm}^{-3}\ \text{sec}^{-1} \tag{3}$$

The rates of the inverse processes, excitation and deexcitation, are equal provided that the sum of the frequencies for superelastic collisions from each state K to all possible states L is larger than the sum of the Einstein coefficients, which are the transition probabilities for radiative emission from the upper state. This condition defines detailed balancing, according to which, if a Maxwellian distribution of electrons is assumed, the deexcitation rate r_{dex} between any two states is equal to the excitation rate r_{ex}. The deexcitation rate from state K to state L can be written

$$r_{dex} = N_e N_K \left(\frac{\omega_L}{\omega_K}\right) e^{\Delta E_{K,L}/k\theta_e} \langle (Q_{L,K})v \rangle \tag{4}$$

where $\dfrac{\langle (Q_{K,L})v \rangle}{\langle (Q_{L,K})v \rangle} = \left(\dfrac{\omega_L}{\omega_K}\right) e^{\Delta E_{K,L}/k\theta_e}$ is the ratio of the deexcitation collision coefficient to the excitation collision coefficient. In equation (4) ω_L and ω_K are the total degeneracies of the levels L and $K = \sum_J (2J + 1)$.

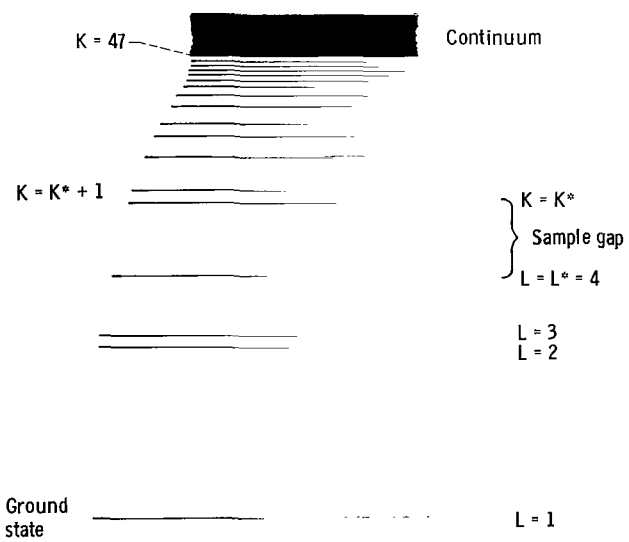

Figure 1. - Schematic energy level diagram for cesium atom that shows sample gap.

The rate of deexcitation R_{dex} across a gap $K^* \rightarrow L^*$ is the sum of the rates at which K^* and all states K above the state K^* can be deexcited by superelastic collision either past the state L^* to all states L below L^* or to the state L^*. Figure 1 schematically displays the arrangement of energy levels and gaps for cesium below the electron continuum, which is indicated by the

solid dark area. The rate R_{dex} can be written

$$R_{dex} = \sum_{K=K^*}^{K=N} \sum_{L=1}^{L=L^*} r_{dex} \tag{5}$$

where all states K are above K^* and all states L are below L^* as indicated in the figure, and N, the total number of states, is equal to 47.

In all cases, the population (cm^{-3}) N_K of the state K is given by the Saha equation since, as mentioned, the bound states are assumed to be in equilibrium with the free electrons. Each population is given by

$$N_K = \frac{\omega_K}{\omega_e \omega_i} \left(\frac{h^2}{2\pi m_e k\theta_e} \right)^{3/2} e^{E_K/k\theta_e} N_e^2$$

where E_K is the binding energy of level K (its previously introduced E_1 value), ω_e is 2 for the free electron, and ω_i is 1 for the degeneracy of the cesium ion.

Estimation of γ. - The value of γ in the relation $R_{rec} = \gamma(R_{dex})_{min}$ is an indication of the magnitude of nonequilibrium effects (refs. 1 and 3) and is a function of electron temperature. This factor must account for the fraction of the minimum deexcitation rate that is balanced by excitation as the system approaches equilibrium, as well as for nonequilibrium populations.

The deexcitation fraction as well as the excitation and deexcitation cross sections for important transitions across the gap are calculated by comparing relaxation times required to attain equilibrium for states above and below the minimum. The ratio of these cross sections contains the factor $(\omega_L/\omega_K)e^{\Delta E_{L,K}/k\theta_e}$ where $\Delta E_{L,K}$ is the energy difference and the ω values are the degeneracies for the significant transitions.

At the lower electron temperatures, where the rate-controlling gap is located between high quantum states, neither capture rates nor state populations differ much for adjoining states above and below the gap, consequently, reexcitation is important. The energy differences for important transitions are less than $k\theta_e$, so that the excitation cross section is usually comparable to the deexcitation cross section. Therefore, for low electron temperatures, 500° to 3000° K, the deexcitation fraction must first be determined by detailed examination of the significant excitation cross sections, and then the populations of the states above the gap are corrected for their departure from equilibrium values to obtain the γ factor.

At high temperatures, where the (6p → 6s) gap controls the rate process, capture rates are very different for states above the gap and the ground state, so that the deexcitation fraction is near unity and γ must account only for the inaccurate populations of the 6p state and several states above it.

In either case any inaccuracy involved in estimating γ is well within the error due to the collision cross sections. These considerations yield estimates for γ of 1/3 up through 2000° K, 1/2 from 3000° to 5000° K, and 2/3 for 5000° to 10,000° K.

RESULTS AND DISCUSSION

The plot of $R_{dex}(cm^{-3}\ sec^{-1})$ against the mean gap energy, $E^* = E_K + \frac{1}{2}(E_L - E_K)$ calculated from equations (4) and (5), is given in figure 2 for θ_e = 1000° K and $N_e = 10^{15}$ per cubic centimeter. The values for these energy gaps are given in table II. The dashed curve is a similar plot from reference 1 for potassium and shows a more regular behavior than the points obtained in the present study. It should be noted that Byron, et al. (ref. 1) assumed that the levels above, as well as below, L^* are continuous rather than discrete and also that the slope of the Gryzinski cross section can be approximated by a linear function in the range of θ_e from 500° to 2000° K. There is more quantum fine structure in the results of this study although the minimum R_{dex} (which gives R_{rec}) is not too different in E^* value from reference 1. This agreement is expected since these two alkalis have qualitatively similar arrangements of atomic energy levels.

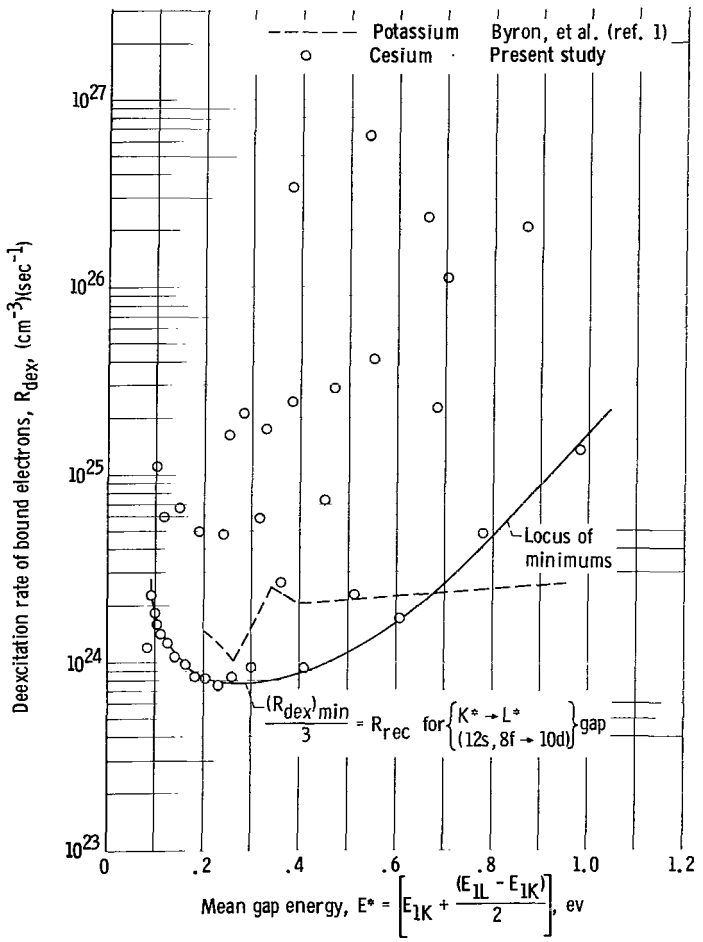

Figure 2. - Deexcitation rate as function of mean gap energy. Electron number density, 10^{15} per cubic centimeter; free-electron temperature, 1000° K.

The locus of minimums in figure 2 denotes the gaps $K^* \rightarrow L^*$ that have the lowest R_{dex} values in the various ranges of E^* at θ_e = 1000° K. The recombination rate is one-third the value of the minimum of the locus curve, which occurs in this case for the (12s, 8f → 10d) gap at E^* = 0.23 electron volt.

Figure 3 shows the recombination rate R_{rec} as a function of electron temperature θ_e in the range 500° to 10,000° K. It is clear that the location of the rate-limiting mean gap energy E^* is depressed with increasing tempera-

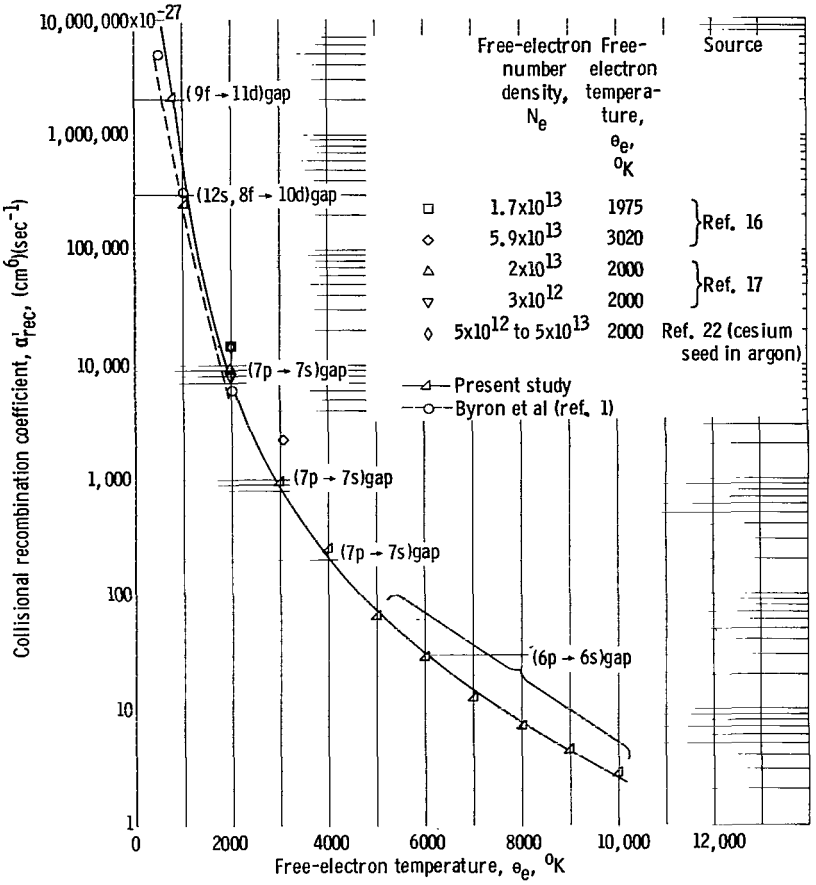

Figure 3. - Three-body collisional recombination coefficient as function of free-electron temperature for range of electron number density 10^{13} to 10^{18} per cubic centimeter.

ture. It should be noted that the (6p → 6s) energy difference results in a relatively long time for the ground state to come to equilibrium so the deexcitation is only slightly balanced by excitation. At temperatures above 10,000° K, two-body radiative recombination becomes important along with quantum effects, so that the purely collisional form of $\alpha' = R_{rec}/N_e^3$ is no longer adequate.

The temperature dependence in the range 500° to 2000° K is much the same as the dashed curve shown for the work of Byron, et al. (ref. 1) in figure 3. This temperature coefficient α' is similar to the α of reference 2, which is a treatment of a quite different nature from the present calculation. Additional calculations that were performed with 59 discrete energy levels showed that "collapse" of energy levels separated by small gaps, which produces new ω values, changes the calculated rates by only several percent at most. The temperature dependence of α' goes from θ_e^{-5} in the range 500° to 3000° K to $\theta_e^{-9/2}$ in the range of θ_e from 4000° to 10,000° K compared with the $\theta_e^{-9/2}$ dependence of reference 5.

The results shown in figure 3 are in good agreement (within a factor of 2) with the experimental findings of reference 20 for a cesium plasma with N_e values from 1×10^{12} to 6×10^{13} per cubic centimeter and θ_e values from 0.11 to 0.26 electron volt. They also agree closely with the data of reference 21 taken for a pure thermal cesium plasma in the ranges of N_e of 5×10^{12} to 10^{13} per cubic centimeter and θ_e of 2000° to 2500° K. Since both radiative deexcitation and trapping of resonance radiation occur in these plasmas for N_e values of interest, it is pointless to offer a refined interpretation of the difference between experiment and theory.

The theoretical results are also in good agreement with the low electron

temperature experimental data of reference 22 for an argon plasma seeded with cesium, which is in excellent agreement with the theoretical value of reference 5.

The recombination results for a modified D'Angelo approach (ref. 4) are shown for comparison in figure 4. This supplementary calculation was done in

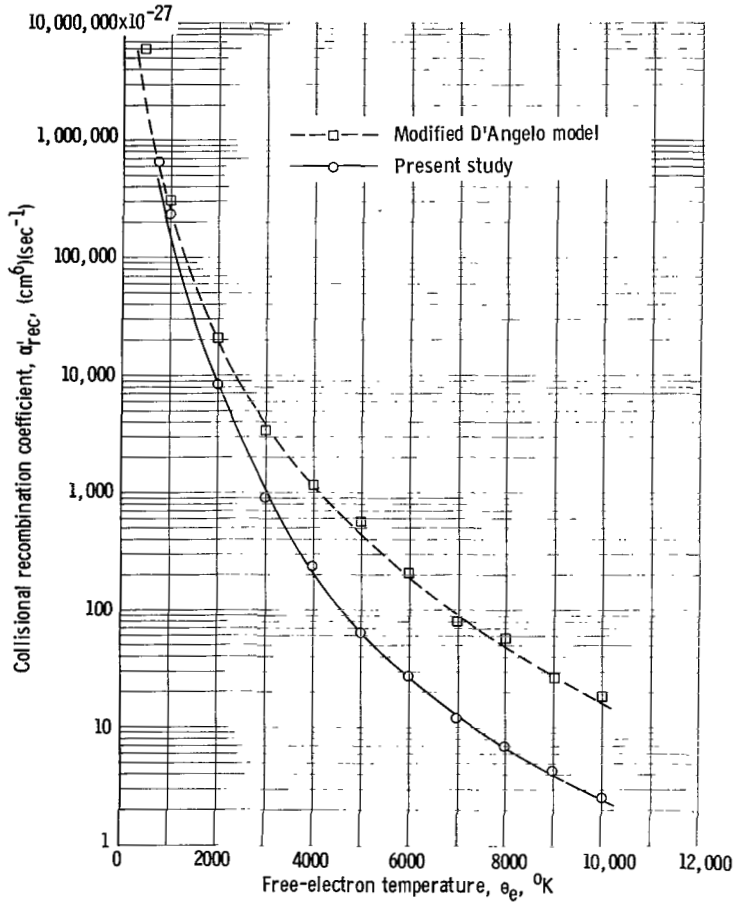

Figure 4. - Comparison of recombination rate as function of electron temperature between Byron approach and modified D'Angelo model for cesium.

a manner quite different from the Byron approach and is outlined in appendix C.

CONCLUDING REMARKS

For conventional output power densities of the magnetohydrodynamic generator, recombination could be a problem, especially below free-electron temperatures of 3000° K because of the strong inverse temperature dependence of the net recombination rate. However, as others have suggested (Byron, et al.) with the use of electron beams to "kick up" the electron temperature initially, the induced field in the generator may then provide "sustained" electron heating to keep the electrons at an elevated temperature, thus avoiding the harmful recombination losses. With the "hot" electrons (electron temperature >> gas temper-

ature) the cesium seeded argon system remains the most promising one for obtaining high conductivity at optimum operating conditions in view of the fact that the net recombination rates calculated for plasmas of interest are not prohibitive.

Although the accuracy of the method is limited by the cross section expressions that underestimate the excitation rate and, consequently, the deexcitation rate, it may be possible to ascribe differences between experiment and theory to radiation effects in the plasma. For example, if the observed recombination rate is significantly less than the theoretical rate, the difference may be attributed to radiation trapping. The method does provide a straightforward approach for estimating net recombination and has been remarkably successful thus far.

The computer program for the recombination calculation is included in appendix D with explanatory remarks. For any number densities or electron temperatures, the only additional data required are the energy levels, E_l values, and corresponding degeneracy values ω for the atom of interest. The γ factor can be estimated as described in the text.

Lewis Research Center
National Aeronautics and Space Administration
Cleveland, Ohio, July 27, 1964

APPENDIX A

SYMBOLS

A_{KL} Einstein coefficient for emission between states K and L, sec^{-1}

C_0 normalization factor for Maxwellian distribution

ΔE inelastic energy loss for collision, ev

E_K binding energy of level K, E_{1K}, ev

E_1 kinetic energy of bound electron (ionization potential of atomic state), ev

E_2 kinetic energy of incident electron, ev

E^* mean binding energy of quantum gap, ev

e unit electronic charge, 4.8×10^{-10} esu

h Planck's constant, 4.1×10^{-15} (ev)(sec)

$\hbar$ $h/2\pi$

J spin orbit quantum number, $l \pm S_p$

K electronic energy level above gap; K^* the electronic energy level immediately above gap

k Boltzmann's constant, 8.6×10^{-5} (ev)($^oK^{-1}$)

L electronic energy level below gap; L^* the electronic energy level immediately below gap

l secondary (orbital angular momentum) quantum number

M neutral mass, 6.8×10^{-23} g (argon), 2.2×10^{-22} g (cesium)

m_e electronic mass, 9.1×10^{-28} g

N_e free-electron number density, cm^{-3}

N_K population of state K, cm^{-3}

N_L population of state L, cm^{-3}

N_+ ion number density, N_e, cm^{-3}

n principal quantum number

Q_{ee} electron-electron collision cross section for momentum transfer, cm^2

Q_{en} electron-neutral collision cross section for momentum transfer, cm^2

R_{dex} deexcitation rate of bound electrons, $(cm^{-3})(sec^{-1})$

R_{ex} excitation rate of bound electrons, $(cm^{-3})(sec^{-1})$

R_{rec} net recombination rate, $(cm^{-3})(sec^{-1})$

S_p total spin quantum number, 1/2 for all cesium atom states

v_{ee} electron-electron relative velocity, $(cm)(sec^{-1})$

v_{en} electron-neutral relative velocity, $(cm)(sec^{-1})$

w free-electron kinetic energy, ev

α' collisional recombination coefficient, $(cm^6)(sec^{-1})$

γ adjustment factor to account for absence of complete bound-free equilibrium and reexcitation effects

θ_e temperature of free electrons, ^oK

σ_o cross section constant, 6.53×10^{-14} $(cm^2)(ev^2)$

ν_{ee} electron-electron collision frequency for momentum transfer, sec^{-1}

ν_{en} electron-neutral collision frequency for momentum transfer, sec^{-1}

ω_K statistical weight (total degeneracy) of an electronic level K, $\sum_J (2J + 1)$

APPENDIX B

NEGLECT OF RADIATION

The extent to which radiative emission can be neglected as a deexcitation mechanism can be assessed from table III, which lists the superelastic collision frequencies $\Sigma\nu_{sek}$ (sec^{-1}) for all deexcitation collisions from a state K. Each frequency is a reciprocal of the superelastic relaxation time. This quantity $\Sigma\nu_{sek}$ is the total frequency for deexcitation across a gap $K^* \rightarrow L^*$ from a state K for N_e of 10^{15} per cubic centimeter and θ_e of 5000° K. In comparison, the oscillator strengths for cesium radiation emission are relatively small for transitions between excited states, while transitions to the ground state have a maximum frequency A_{KL} of 3×10^7 per second (ref. 23). Most of the Einstein coefficients A_{KL} are at least an order of magnitude less than this maximum. Since $\Sigma\nu_{sek}$ is much greater than ΣA_{KL} it appears that radiative deexcitation will only become significant for N_e less than 3×10^{14} per cubic centimeter at even the lowest electron temperatures.

APPENDIX C

MODIFIED D'ANGELO MODEL

A separate approach to the recombination rate was made in this study with a modification of the D'Angelo model. Reference 4 outlines a treatment whereby electrons are traced from the continuum after being captured in a three-body process at a rate R_{cap}; however, the only downward process included between electronic levels was radiative transition and the only upward process included was collisional ionization. This study includes superelastic collisions and excitation collisions. The inclusion of these processes leads to a divergent recombination rate if Bohr-Thomson cross sections (see ref. 16) are employed. This occurs because capture is the limiting step with the inclusion of collisional processes in the modified model. The capture rate naturally diverges for increasing orbital size and decreasing ionization potential or binding energy; however, if the bound state distribution is fitted to the Maxwellian distribution in the manner of a continuous function, as suggested by John E. Heighway of Lewis, a cutoff is derived for the bound states at $3/2\ (k\theta_e)$, the average of the free-electron energies. The recombination rate is then calculated by summing over all states below the cutoff.

APPENDIX D

COMPUTER PROGRAM FOR STUDYING RECOMBINATION OF AN ATOMIC ION

by Lynn U. Albers

The computer program was written in FORTRAN IV compiler language for execution on an IBM 7094 computer under control of the Lewis IBSYS Monitor System. It consists of a main program, an integration subroutine VQEXI, and a function subprogram F.

The purpose of the main program is to compute the following three sums for all (L^*,K^*) gaps where $K^* = L^* + 1$ and L^* varies from 1 to the number of states N:

$$\text{RDEX} = \sum_{L=1}^{L^*} \sum_{K=K^*}^{N+1} F_1(L,K) \tag{D1}$$

$$\text{F2SUM} = \sum_{L=1}^{L^*} \sum_{K=K^*}^{N+1} F_2(L,K) \tag{D2}$$

$$\text{DEXF} = \sum_{L=1}^{L^*} F_2(L,K^*) \tag{D3}$$

where

$$F_1(L,K) = N_K F_2(L,K) \tag{D4}$$

and

$$F_2(L,K) = P_3\left[I(E_L, E_L - E_K) - I(E_L, E_L - E_{K+1})\right] \qquad \text{if} \quad K \leq N$$

$$= P_3 I(E_L, E_L) \qquad \text{if} \quad K = N + 1 \tag{D5}$$

are equations related to equations (2) and (4) in the text. The parameter P_3 is one of three parameters defined by

$$P_1 = \frac{\sigma_0 8\pi}{C_0} N_e \tag{D6}$$

$$P_2 = N_e^2 \left(\frac{h^2}{2\pi m_e k \theta_e}\right)^{3/2} \tag{D7}$$

$$P_3 = P_3(L,K) = \frac{P_1 \omega(L) e^{\Delta E/k\theta_e}}{\omega(K)} \qquad \text{where} \quad \Delta E = E_L - E_K \tag{D8}$$

The parameter P_2 is used in the formula for the population of the state K:

$$N_K = P_2 \omega(K) e^{E_K/k\theta_e} \tag{D9}$$

The integral I of equation (D5) is computed in the subroutine VQEXI and is defined by

$$I(E_1,\Delta E) = \frac{1}{(\Delta E)^2} \int_{\Delta E}^{0.1\ \theta_e} G(E_2,E_1,\Delta E) F(E_1,E_2) E_2\ dE_2 \tag{D10}$$

by using the notation of equations (1a), (1b), and (2). In this subroutine, the whole integrand is denoted by $F(E_2)$ with E_1 and ΔE being available in COMMON. Since some factors in the integrand are likely to be smaller than the 10^{-38} limit for single-precision floating-point numbers, precaution is taken to compute a BIAS for the exponent, which is stored in COMMON and used to bias the argument of the exponential function every time the integrand is computed by means of the subprogram F. A compensating scale factor SCAL is included in the P_3 formula for PAR3. The integration is performed by Simpson's Rule in the routine VQEXI. The integrand has the character of varying widely in a very narrow domain at the left of the interval and being negligible elsewhere. The VQEXI routine searches for this narrow interval where the integrand is greater than 10^{-5} times $F(\Delta E)$ and uses 32, 64, or 128 integration steps to evaluate the integral.

The Grysinski expressions for $\Delta E = E_2$ give falsely negative integrands, which might throw some doubt on end-point formulas. However, even internal formulas like Gaussian quadrature formulas gave the same results, so no error is involved in the method used. The logic of the VQEXI routine is simple enough that it could be replaced by some other process if further improvement in execution time is desired.

After the reading in of energy levels and their identification numbers, as well as conditional input of modified omegas, all parameters independent of temperature and electron number density are computed. The remainder of the program accomplishes an iterative input of a temperature and an electron density and a calculation of an output of the sums defined in equations (D1), (D2), and (D3).

An earlier version of the program computed the sum for each gap separately. Since for gaps near the middle this would involve the sum of many terms, and the computations for adjacent gaps overlap considerably, the program was modified to compute the sum for one gap from the sum for the preceding gap by making proper additions and subtractions. When this was first done, each

addend was computed as needed, once when added, and again when subtracted. By storing each addend the first time it was computed, the execution time could be halved. The disadvantage of proceeding by augmentation and deletion is that sums near the end of the process, though composed of a relatively small number of terms, are masked by the round-off error attendant on adding and subtracting large terms. Hence, a provision is made for recomputing gap sums from the low end conditionally for a number of steps.

If one wishes to shorten execution time by neglecting terms between widely separated states, one can by changing LKD, limit LL to being greater than L^* - KLD, and limit KK to being less than K^* + LKD. This, in effect, truncates the sums in equations (D1) and (D2).

As RDEX and F2SUM are computed for each gap, starting at the low end, they are listed alongside of the labels for L^* and K^*, the L^* and K^* indices, and the population N_{K^*} of the upper state. Then if NBW is positive, gap sums are recomputed and listed starting from the high end for the required number of steps by using the F2 terms stored earlier. The table TAB has five rows of 99 elements each. F2SUM and RDEX in the forward sweep are stored in rows 1 and 2. F2SUM and RDEX recomputed in the backward sweep are stored in rows 3 and 4. Finally, the DEXF is computed and stored in row 5. If a TABLE 1 value is negative, this indicates round-off error for this and all higher gaps, and TABLES 1 and 2 are overwritten by the more accurate TABLES 3 and 4 from this gap to the top gap. It may be necessary to recompute the tables for a large number of states from the high end at lower electron temperatures (e.g., NBW = 43 at $\theta_e = 1000^\circ$ K) while at higher temperatures, that is, 5000° K and above, no recomputation is necessary.

Once this table has been assembled, it is read out in two sections called table II and table III. Table II lists F2SUM, RDEX, and the average ionization potential for the gap in sets of twenty in such a way that each sum is bracketed by the labels and N_K's of the bounding states of its gap. Table III lists DEXF and RDEX in corresponding sets of twenty. After this is done, a new (θ_e, N_e) pair is read in until all cases are treated.

Following is an outline of the main program using FORTRAN symbols. A dictionary of these symbols with their meanings is given after the outline, and finally a listing of (1) MAIN, (2) VQEXI, (3) F, and (4) a typical set of data.

OUTLINE OF MAIN

I. Specify constants PI, K, H, SIGZ, and ME.

II. Specify atomic data GSIP, NSTAT, WE, and LKD.

III. Read in arrays LAB, EN, and OMEGA.

IV. List OMEGA array, GSIP, WE, and EN array.

V. Provide for states beyond N^{th}.

VI. Compute IP array (loop 1) and list it.

VII. Read in NE, THETA, NBW and list them.

VIII. Calculate KT, KTHET, PAR1, PAR2, and INF.

IX. Compute NK array (loop 2) and list it.

X. Calculate BIAS and SCAL.

XI. Skip to next page and print headings at top. Set F2SUM and RDEX to zero.

XII. Make forward sweep calculating and storing F2SUM and RDEX for each gap in TAB matrix, and listing them and associated data line by line (loop 3). LSTAR runs from 1 to NSTAT.

A. Compute KSTAR, KMAX, LMIN, and E1.

B. Augment sums by proper terms for this gap (loop 4) KK = KSTAR to KMAX.

1. Compute DELE, PAR3 for (L*,KK) pair.

2. Do first integral (see eq. (D5)) and store in TERM.

3. Conditionally compute the second integral for (L*,KK + 1) pair and subtract it from TERM to get F2 value.

4. Increment F2SUM, RDEX. Store F2 element in (L*,KK) slot.

C. Subtract proper terms from sums for this gap (loop 5) LL = LMIN to L* - 1.

1. Obtain F2(LL,L*) from storage.

2. Decrement F2SUM and RDEX.

D. Store final F2SUM and RDEX in Tables 1 and 2 in L* slot.

E. List LAB(L*), LAB(K*), L*, K*, F2SUM, RDEX, NK(K*).

XIII. Calculate DEXF array and store in Table 5 (loop 6) KK = 2 to NSTAT + 1.

A. Set DEXF to zero.

B. Accumulate in DEXF sum of F2(LL,KK) for LL = 1 to KK - 1 (loop 7).

C. Store DEXF in Table 5 at slot KK - 1.

XIV. Conditionally recalculate F2SUM and RDEX in NBW section storing results in Tables 3 and 4 (loops 23 and 25).

A. List heading for this backwards section.

B. (Loop 23) Recalculate F2SUM and RDEX from equations (D1) and (D2) for L^* = NSTAT down to NSTAT - 5 by using stored F2 values. This uses loop 24. List results as in XII.E. Store results in TABLES 3 and 4.

C. (Loop 25) Continue recalculation of F2SUM and RDEX for total of NBW gaps, but this time use proper augmentation and deletion, as in loop 3. This uses loops 26 and 27, lists results, as in XII.E., and stores results in TABLES 3 and 4.

D. Search last NBW entries in TABLE 1 to find the lowest gap with negative entry (loop 28).

E. Overwrite TABLE 1 with TABLE 3, and TABLE 2 with TABLE 4 for this gap and higher gaps (loop 29).

XV. List TABLE 5 entries, six per row (loop 8).

XVI. List tables II and III alternately in sets of twenty gaps per page starting from the high end (loop 9).

A. Page 1 - Last twenty gaps - table II (loop 21).

B. Page 2 - Last twenty gaps - table III (loop 22).

C. Page 3 - Next to last twenty gaps - table II (loop 21).

D. Page 4 - Next to last twenty gaps - table III (loop 22).

E. Page 5 - Remaining gaps - table II (loop 21).

F. Page 6 - Remaining gaps - table III (loop 22).

XVII. Skip page. Return to step VII.

DICTIONARY OF SYMBOLS

BIAS- BIAS IN EXPONENT NECESSARY TO KEEP INTEGRAND IN RANGE
DELE- DELTA E OR IP(L)-IP(K) NEEDED IN VQEX INTEGRATION
DEXF DEEXCITATION FREQUENCY. SEE EQUATION D3
E1- IONIZATION POTENTIAL FOR L STATE IN VQEX CALCULATION
EN ENERGY LEVEL FOR STATE IN RECIPROCAL CENTIMETERS
F2 FUNCTION 2 DEFINED BY BY EQUATION D5
GSIP- GROUND STATE IONIZATION POTENTIAL
H- PLANCKS CONSTANT IN ERG-SECONDS
INF- INFINITY FOR VQEX INTEGRATION
IP- IONIZATION POTENTIAL IN ELECTRON VOLTS
K- K IN ERGS PER DEGREE KELVIN
KSTAR-K* THE INDEX OF THE UPPER GAP LIMIT
KTHET-K TIMES THETA IN ELECTRON VOLTS
LAB LABEL FOR A STATE
LKD- LIMIT ON L-K DIFFERENCE TO SHORTEN EXECUTION TIME
LSTAR-L* THE INDEX OF THE LOWER GAP LIMIT
ME- MASS OF ELECTRON IN GRAMS
NBW- NUMBER OF BACKWARD STEPS TO TAKE IN GAP CALCULATIONS
NE ELECTRON DENSITY
NK- POPULATION OF STATE
NSTAT-NUMBER OF STATES
OMEGA-TOTAL DEGENERACY FOR STATE
PAR1- PARAMETER 1 DEFINED IN EQUATION D6
PAR2- PARAMETER 2 DEFINED IN EQUATION D7
PAR3- PARAMETER 3 DEFINED BY EQUATION D8
SCAL- SCALE FACTOR TO COUNTERACT BIAS AFTER INTEGRATION
SIGZ- SIGMA ZERO IN CM SQR-EV SQR
TAB- TABLE FOR SUMMARY PURPOSES
TABLE 1 F2SUM FROM FORWARD SWEEP. SEE EQUATIONS D2 AND D5
TABLE 2 RDEX FROM FORWARD SWEEP. SEE EQUATIONS D1 AND D4
TABLE 3 F2SUM RECALCULATED IN NBW SECTION
TABLE 4 RDEX RECALCULATED IN NBW SECTION
TABLE 5 DEXF DEFINED IN EQUATION D3
THETA-TEMPERATURE IN DEGREES KELVIN
WE OMEGA ELECTRON

PROGRAM LISTING

```
$IBFTC MAIN     DECK
C      PROGRAM FOR STUDYING RECOMBINATION OF AN ATOMIC ION
       DIMENSION LAB(100),EN(100), OMEGA(100),F2(99,99),NK(99),IP(99)
       COMMON E1,KTHET,BIAS,DELE
       DIMENSION TAB(5,99)
       REAL     NE,NK,IP,INF,KTHET,K,ME, KT,NKS
       PI=3.1415927
       K=1.38E-16
       H=6.625E-27
       SIGZ=6.53E-14
       ME=9.1E-28
       GSIP=31407.
       NSTAT=47
       WE=2.
       LKD=99
       READ (5,20) (LAB(J),EN(J),J=1,NSTAT)
 20    FORMAT (6(I5   ,F7.0))
       READ (5,30)    (OMEGA(J),J=1,NSTAT)
 30    FORMAT (24F3.0)
       WRITE (6,40) (OMEGA(J),J=1,NSTAT),GSIP,WE
       WRITE (6,40) (EN(J),J=1,NSTAT)
 40    FORMAT (3X,10F9.1)
       N=NSTAT
       NP1=N+1
       NP2=N+2
       OMEGA(NP1)=10.
       LAB(NP1)=999
       EN(NP1)=GSIP
       EN(NP2)=GSIP
       DO 1 J=1,NP2
  1    IP(J)=(GSIP-EN(J))/8067.
       WRITE (6,50) (IP(J),J=1,NP2)
 50    FORMAT (4H IP  1P9E12.5)
 11    READ  (5,10) NE,THETA,NBW
 10    FORMAT (F10.0,F5.0,4I5)
       NE=NE*1.E+13
       WRITE (6,60)     THETA,NE,NBW
 60    FORMAT (1H1/5X,7HTHETA= , F11.4,20X,4HNE= 1PE10.1,I8)
       KT=K*THETA
       KTHET=KT/1.6E-12
       PAR1=1.30035E-24*NE/KT*SIGZ/SQRT(KT)*PI/SQRT(ME)
       X=(H/KT)*(H/ME)/(2.*PI)
       PAR2=NE*NE*X*SQRT(X)/WE
       INF=.01*THETA
       DO 2 J=1,NP1
  2    NK(J)=PAR2*OMEGA(J)*EXP(IP(J)/KTHET)
       WRITE (6,70) (NK(J),J=1,NP1)
 70    FORMAT   (3H XN 1P9E12.4)
C     SECTION TO KEEP INTEGRAND IN RANGE FOR LOWEST GAP
       BIAS=0.
       EXPON=-IP(1)/KTHET
 12    IF(EXP(EXPON)) 13,13,14
 13    BIAS=BIAS+10.
       EXPON=EXPON-10.
       GO TO 12
 14    SCAL=1.E-10*EXP(-BIAS)
C     MAIN LOOP FOR COMPUTING RDEX SUMS FROM LOWEST TO HIGHEST GAP
       WRITE (6,80)
```

```
 80       FORMAT (43H1 GAP  L* K*    F2SUM    RDEX    NK(K*)
          F2SUM=0.
          RDEX=0.
          DO 3 LSTAR=1,N
          KSTAR=LSTAR+1
          KMAX=KSTAR+LKD
          IF (KMAX.GT.NP1)   KMAX=NP1
          LMIN=LSTAR-LKD
          IF (LMIN.LT.1)  LMIN=1
C     LOOP FOR ADDING AND COMPUTING LSTAR-K TERMS
          E1=IP(LSTAR)
          DO 4 KK=KSTAR,KMAX
          DELE=IP(LSTAR)-IP(KK)
          PAR3=PAR1*SCAL*OMEGA(LSTAR)/OMEGA(KK)*EXP(DELE/KTHET)
          CALL VQEXI(DELE,INF,ANS)
          TERM=ANS*PAR3/DELE**2
          DELE=IP(LSTAR)-IP(KK+1)
          IF (KK.GT.NSTAT)  GO TO 15
          CALL VQEXI(DELE,INF,ANS)
          TERM=PAR3*ANS/DELE**2-TERM
 15       TERM=ABS(TERM)
            F2(LSTAR,KK)=TERM
          F2SUM=F2SUM+TERM
          RDEX=RDEX+TERM*NK(KK)
  4       CONTINUE
C     LOOP FOR SUBTRACTING PROPER L-KSTAR TERMS
          LM1=LSTAR-1
          IF (LM1.LT.1)  GO TO 16
          DO 5 LL=LMIN,LM1
          TERM=  F2(LL,LSTAR)
          F2SUM=F2SUM-TERM
          RDEX=RDEX-TERM*NK(LSTAR)
  5       CONTINUE
 16       TAB(1,LSTAR)=F2SUM
          TAB(2,LSTAR)=RDEX
          NKS=NK(KSTAR)
  3       WRITE (6,90)LAB(LSTAR),LAB(KSTAR),LSTAR,KSTAR,F2SUM,RDEX,NKS
 90       FORMAT (2A9,2I5,1P4E22.4)
C     SECTION FOR PUTTING OUT SUMMARY TABLES
          DO 6 KK=2,NP1
          DEXF=0.
          DO 7 LL=2,KK
  7       DEXF=DEXF+F2(LL-1,KK)
  6       TAB(5,KK-1)=DEXF
          IF (NBW.LE.0)  GO TO 19
C      NBW SECTION FOR RECALCULATION OF RDEX AND F2SUM FROM HIGH GAP END
          WRITE (6,35) NBW
 35       FORMAT (20H  BACKWARDS SECTION  I5,6H STEPS )
          DO 23 J=1,6
          I=NP1-J
          F2SUM=0.
          RDEX=0.
          JP=I+1
          DO 24 KK=JP,NP1
          NKS=NK(KK)
          DO 24 L=1,I
```

```
          TERM=F2(L,KK)
          F2SUM=F2SUM+TERM
   24     RDEX=RDEX+TERM*NKS
          TAB(3,I)=F2SUM
          NKS=NK(JP)
          TAB(4,I)=RDEX
   23     WRITE (6,90) LAB(I),LAB(JP),I,JP,F2SUM,RDEX,NKS
          DO 25 J=7,NBW
          I=NP1-J
          JT=I+2
          JP=I+1
          NKS=NK(JP)
          DO 26 L=1,I
          TERM=F2(L,JP)
          F2SUM=F2SUM+TERM
   26     RDEX=RDEX+TERM*NKS
          DO 27 KK=JT,NP1
          TERM=F2(JP,KK)
          F2SUM=F2SUM-TERM
   27     RDEX=RDEX-TERM*NK(KK)
          TAB(3,I)=F2SUM
          TAB(4,I)=RDEX
   25     WRITE (6,90) LAB(I),LAB(JP),I,JP,F2SUM,RDEX,NKS
C     REPLACE TABLE 1 AND 2 VALUES WITH BETTER ONES WHEN AVAILABLE
          JT=0
          DO 28 J=1,NBW
          L=NP1-J
          IF (TAB(1,L).GE.0.)  GO TO 28
          JT=L
   28     CONTINUE
          IF (JT.LE.0)  GO TO 19
          DO 29 L=JT,N
          TAB(1,L)=TAB(3,L)
   29     TAB(2,L)=TAB(4,L)
   19     DO 8 JA=1,NSTAT,6
          JB=JA+5
    8     WRITE (6,31) JA,(TAB(5,J),J=JA,JB)
   31     FORMAT (3X,I5,1P6E14.5)
          KA=NSTAT-19
          DO 9 JA=1,NSTAT,20
          KW=2
          KB=KA+20
          WRITE (6,32)  KB,KW
   32     FORMAT (6H1  K=  I2,I5//2H    )
          WRITE (6,33) LAB(KB),NK(KB)
   33     FORMAT (5X,I5,28X,1PE14.2)
          DO 21 JB=1,20
          KB=KB-1
          IF (KB.LT.1) GO TO 17
          AVIP=.5*(IP(KB)+IP(KB+1))
          WRITE (6,34)  TAB(1,KB),TAB(2,KB),AVIP
   34     FORMAT (10X,1P2E14.2,14X,0PF9.3)
          WRITE (6,33) LAB(KB),NK(KB)
   21     CONTINUE
   17     KW=3
          KB=KA+20
```

```
      WRITE (6,32)  KB,KW
      WRITE (6,33) LAB(KB),NK(KB)
      DO 22 JB=1,20
      KB=KB-1
      IF (KB.LE.0)  GO TO 18
      WRITE (6,34)  TAB(5,KB),TAB(2,KB)
      WRITE (6,33) LAB(KB),NK(KB)
22    CONTINUE
 9    KA=KA-20
18    KW=2
      WRITE (6,32)  KB,KW
      GO TO 11
      END


$IBFTC VQEXI
      SUBROUTINE VQEXI (XL,XU,ANS)
      X=XL
      Y=XU
      D=(Y-X)/512.
      XA=X+D
      E=1.E-5*ABS(F(X))
12    IF (ABS(F(XA)).LT.E) GO TO 11
      XA=XA+D
      IF (XA.LT.Y)   GO TO 12
11    Y=XA-D
      D=(Y-X)/32.
      D2=D+D
      N=16
      T=X+D2
      S=F(T)
      DO 1 J=3,N
      T=T+D2
 1    S=S+F(T)
      A=(F(X)+F(Y)+2.*S)*D/3.
      T=X+D
      S=F(T)
      DO 2 J=2,N
      T=T+D2
 2    S=S+F(T)
      B=4.*S*D/3.
      R=A+B
      E=.00001*ABS(R)
      IF (E) 5,5,7
 7    DO 3 J=1,2
      C=.5*(A+1.5*B)
      D2=D
      D=.5*D
      N=2*N
      T=X+D
      S=F(T)
      DO 4 K=2,N
      T=T+D2
 4    S=S+F(T)
      B=4.*S*D/3.
```

```
          A=R-C
          R=A+B
          W=ABS(B-C)
          IF (W-E) 5,5,3
  3       CONTINUE
  5       ANS=R
          RETURN
          END


$IBFTC F
          FUNCTION F(ARG)
          COMMON E1,KTHET,BIAS,DELE
          REAL KTHET
          E2=ARG
          IF (C6.GT.0.) GO TO 3
          C6=2./3.
  3       E1E2=E1/E2
          DEE2=DELE/E2
          E2ES=E2/(E1+E2)
          IF ((DELE+E1).GT.E2)   GO TO 2
C     EQUATION 1A
          G=C6*E1E2+DEE2*(1.-E1E2)-DEE2**2
          GO TO 4
C     EQUATION 1B
  2       G=C6*(E1E2+DEE2*(1.-E1E2)-DEE2**2)*SQRT((1.+DELE/E1)*(1.-DEE2))
  4       F=E2ES*SQRT(E2ES)*G*EXP(BIAS-E2/KTHET)*E2*1.E10
          RETURN
          END
```

SAMPLE DATA

```
$DATA
  600       0  601  11178  601  11732  502  14499  502  14597  700  18535
  701   21766  701  21947  602  22589  602  22631  800  24317  403  24472
  801   25709  801  25792  702  26048  702  26069  900  26911  503  26971
  504   27010  901  27637  901  27681  802  27816 1000  28300  603  28330
  604   28351 1001  28727 1001  28754  902  28832 1100  29130  703  29148
 1101   29404 1101  29421 1002  29471 1200  29675 1201  29859 1102  29898
  903   30043 1301  30170 1202  30198 1003  30302 1401  30393 1302  30417
 1103   30495 1501  30566 1402  30581 1203  30641 1601  30694
  2  2  4  4  6  2  2  4  4  6  2 14  2  4  4  6  2 14 18  2  4 10  2 14
 40  2  4 10  2 14  2  4 10 16  6 10 14  6 10 14  6 10 14  6 10 14  6
       100 1000   43
       100 5000   00
```

REFERENCES

1. Byron, S., Bortz, P. I., and Russell, G.: Electron-Ion Reaction Rate Theory: Determination of the Properties of Non-Equilibrium Monatomic Plasmas in MHD Generators and Accelerators and in Shock Tubes. Proc. of Fourth Symposium on Eng. Aspects of Magnetohydrodynamics, Univ. Calif., Apr. 10-11, 1963.

2. Bates, D. R., Kingston, A. E., and McWhirter, R. W. P.: Recombination Between Electrons and Atomic Ions. I. Optically Thin Plasmas. Proc. Roy. Soc. (London), ser. A, vol. 267, no. 1330, May 22, 1962, pp. 297-312.

3. Byron, Stanley, Stabler, Robert C., and Bortz, Paul: Electron-Ion Recombination by Collisional and Radiative Processes. Phys. Rev. Letters, vol. 8, no. 9, May 1962, pp. 376-379.

4. D'Angelo, N.: Recombination of Ions and Electrons. Phys. Rev., vol. 121, no. 2, Jan. 15, 1961, pp. 505-507.

5. Hinnov, Einar, and Hirschberg, Joseph G.: Electron-Ion Recombination in Dense Plasmas. Phys. Rev., vol. 125, no. 3, Feb. 1, 1962, pp. 795-801.

6. Talaat, M. E.: Magnetoplasmadynamic Electrical Power Generation with Non-equilibrium Ionization. Paper Presented at Symposium on Magnetoplasmadynamic Electrical Power Generation, King's College, Univ. Durham, Newcastle upon Tyne, Sept. 6-8, 1962.

7. Sutton, G. W.: The Theory of Magnetohydrodynamic Power Generators. Rep. R62SD990, General Electric Co., Dec. 1962.

8. Haught, Alan F.: Shock Tube Investigation of Cesium Vapor. Phys. of Fluids, vol. 5, no. 11, Nov. 1962, pp. 1337-1346.

9. Lyman, Frederic A., Goldstein, Arthur W., and Heighway, John E.: Effect of Seeding and Ion Slip on Electron Heating in a Magnetohydrodynamic Generator. NASA TN D-2118, 1964.

10. Post, Richard F.: Controlled Fusion Research - An Application of the Physics of High Temperature Plasmas. Rev. Modern Phys., vol. 28, no. 3, July 1956, pp. 338-362.

11. Massey, H. S. W., and Burhop, E. H. S.: Electronic and Ionic Impact Phenomena. Clarendon Press (Oxford), 1952.

12. Stone, Philip M., and Reitz, John R.: Elastic Scattering of Slow Electrons by Cesium Atoms. Phys. Rev., vol. 131, no. 5, Sept. 1, 1963, pp. 2101-2107.

13. Gryzinski, Michal: Classical Theory of Electronic and Ionic Inelastic Collisions. Phys. Rev., vol. 115, no. 2, July 15, 1959, pp. 374-383.

14. Fox, R. E.: Ionization Cross Sections Near Threshold by Electron Impact. Jour. Chem. Phys., vol. 35, no. 4, Oct. 1961, pp. 1379-1382.

15. Stabler, Robert C.: Classical Impulse Approximation for Inelastic Electron-Atom Collisions. Phys. Rev., vol. 133, no. 5A, Mar. 2, 1964, pp. A1268-A1273.

16. Robben, Frank, and Kunkel, Wulf B.: Spectroscopic Study of Electron Recombination with Monatomic Ions in a Helium Plasma. Phys. Rev., vol. 132, no. 6, Dec. 15, 1963, pp. 2363-2371.

17. Giovanelli, R. G.: Hydrogen Atmospheres in the Absence of Thermodynamic Equilibrium, pts. I, II, and III. Australian Jour. Sci. Res., ser. A, vol. 1, Sept. 1948, pp. 275-318.

18. Moore, Charlotte E.: Tables of Atomic Energy Levels. Vol. III, NBS, Wash., D.C., 1952.

19. Fowler, R. H.: Statistical Mechanics. Second ed., ch. XVII, Cambridge Univ. Press, 1936.

20. Aleskovskii, Yu. M.: Investigation of Volume Recombination in a Cesium Plasma. Soviet Phys.-JETP, vol. 17, no. 3, Sept. 1963, pp. 570-575.

21. Wada, J. Y., and Knechtli, R. C.: Measurements of Electron-Ion Recombination in a Thermal Cesium Plasma. Phys. Rev. Letters, vol. 10, no. 12, June 15, 1963, pp. 513-516.

22. Harris, L. P.: Ionization and Recombination in Cesium-Seeded Plasmas Near Thermal Equilibrium. Rep. 64-RL-3698G, General Electric Co., June 1964.

23. Roberts, T. G., and Hales, W. L.: Radiative Transition Probabilities and Absorption Oscillator Strengths for the Alkali-Like Ions of the Alkaline Earths and for Calcium I. AMC-RR-TR-62-8, Army Missile Command, Redstone Arsenal, Oct. 23, 1962.

TABLE I. - QUANTUM NUMBERS, IONIZATION POTENTIALS, AND STATISTICAL WEIGHTS OF ELECTRONIC LEVELS USED IN CALCULATIONS

Electronic energy level, K or L	Principal and secondary (orbital) quantum number, n, l	Spin orbit quantum number, J	State binding energy (ionization potential), E_1, ev	Total statistical weight of quantum state (degeneracy), $\omega_K = \sum_J (2J + 1)$	Electronic energy level, K or L	Principal and secondary (orbital) quantum number, n, l	Spin orbit quantum number, J	State binding energy (ionization potential), E_1, ev	Total statistical weight of quantum state (degeneracy), $\omega_K = \sum_J (2J + 1)$
16p,p'	[a]16,1	$\frac{1}{2}, 1\frac{1}{2}$	8.83 E-02	6	10s	[a]10,0	$\frac{1}{2}$	3.85 E-01	2
12f,f'	[a]12,3	$2\frac{1}{2}, 3\frac{1}{2}$	9.49 E-02	14	8d,d'	[a]8,2	$1\frac{1}{2}, 2\frac{1}{2}$	4.45 E-01	10
14d,d'	[a]14,2	$1\frac{1}{2}, 2\frac{1}{2}$	1.02 E-01	10	9p'	9,1	$1\frac{1}{2}$	4.61 E-01	4
15p,p'	[a]15,1	$\frac{1}{2}, 1\frac{1}{2}$	1.04 E-01	6	9p	9,1	$\frac{1}{2}$	4.67 E-01	2
11f,f'	[a]11,3	$2\frac{1}{2}, 3\frac{1}{2}$	1.13 E-01	14	5g,g'	[a]5,4	$3\frac{1}{2}, 4\frac{1}{2}$	5.45 E-01	18
13d,d'	[a]13,2	$1\frac{1}{2}, 2\frac{1}{2}$	1.22 E-01	10	5f,f'	[a]5,3	$2\frac{1}{2}, 3\frac{1}{2}$	5.49 E-01	14
14p,p'	[a]14,1	$\frac{1}{2}, 1\frac{1}{2}$	1.25 E-01	6	9s	[a]9,0	$\frac{1}{2}$	5.57 E-01	2
10f,f'	[a]10,3	$2\frac{1}{2}, 3\frac{1}{2}$	1.36 E-01	14	7d'	7,2	$2\frac{1}{2}$	6.61 E-01	6
12d,d'	[a]12,2	$1\frac{1}{2}, 2\frac{1}{2}$	1,49 E-01	10	7d	7,2	$1\frac{1}{2}$	6.64 E-01	4
13p,p'	[a]13,1	$\frac{1}{2}, 1\frac{1}{2}$	1.53 E-01	6	8p'	8,1	$1\frac{1}{2}$	6.96 E-01	4
9f,f'	[a]9,3	$2\frac{1}{2}, 3\frac{1}{2}$	1.69 E-01	14	8p	8,1	$\frac{1}{2}$	7.06 E-01	2
11d,d'	[a]11,2	$1\frac{1}{2}, 2\frac{1}{2}$	1.87 E-01	10	4f,f'	[a]4,3	$2\frac{1}{2}, 3\frac{1}{2}$	8.59 E-01	14
12p,p'	[a]12,1	$\frac{1}{2}, 1\frac{1}{2}$	1.92 E-01	6	8s	[a]8,0	$\frac{1}{2}$	8.78 E-01	2
8f,f',12s	[a]8,3, [a]12,0	$2\frac{1}{2}, 3\frac{1}{2}, \frac{1}{2}$	2.14 E-01	16	6d'	6,2	$2\frac{1}{2}$	1.07 E-00	6
10d,d'	[a]10,2	$1\frac{1}{2}, 2\frac{1}{2}$	2.40 E-01	10	6d	6,2	$1\frac{1}{2}$	1.09 E-00	4
11p'	11,1	$1\frac{1}{2}$	2.46 E-01	4	7p'	7,1	$1\frac{1}{2}$	1.17 E-00	4
11p	11,1	$\frac{1}{2}$	2.48 E-01	2	7p	7,1	$\frac{1}{2}$	1.19 E-00	2
7f,f'	[a]7,3	$2\frac{1}{2}, 3\frac{1}{2}$	2.80 E-01	14	7s	[a]7,0	$\frac{1}{2}$	1.59 E-00	2
11s	[a]11,0	$\frac{1}{2}$	2.82 E-01	2	5d'	5,2	$2\frac{1}{2}$	2.08 E-00	6
9d,d'	[a]9,2	$1\frac{1}{2}, 2\frac{1}{2}$	3.19 E-01	10	5d	5,2	$1\frac{1}{2}$	2.09 E-00	4
10p'	10,1	$1\frac{1}{2}$	3.28 E-01	4	6p'	6,1	$1\frac{1}{2}$	2.43 E-00	4
10p	10,1	$\frac{1}{2}$	3.32 E-01	2	6p	6,1	$\frac{1}{2}$	2.50 E-00	2
6g,g',h,h'	[a]6,4, [a]6,5	$3\frac{1}{2}, 4\frac{1}{2}, 4\frac{1}{2}, 5\frac{1}{2}$	3.79 E-01	40	6s	[a]6,0	$\frac{1}{2}$	3.89 E-00	2
6f,f'	[a]6,3	$2\frac{1}{2}, 3\frac{1}{2}$	3.81 E-01	14					

[a]Levels degenerate in J value.

TABLE II. - SUPERELASTIC COLLISION FREQUENCIES AND DEEXCITATION RATES ACROSS ELECTRONIC QUANTUM GAPS

[Free-electron number density, 10^{15} cm^{-3}; free-electron temperature, 1000° K.]

Electronic state (47 to 1 inclusive), K	Superelastic collision frequency across gap K* to L*, $\sum_{L=1}^{L=K^*-1} \sum_{K=K^*}^{K=47} \nu_{sek}$, sec^{-1}	Deexcitation rate across gap, K* to L*, R_{dex}, cm^{-3} sec^{-1}	Population of state K, N_K, cm^{-3}	Mean gap energy, E*, ev	Electronic state (47 to 1 inclusive), K	Superelastic collision frequency across gap K* to L*, $\sum_{L=1}^{L=K^*-1} \sum_{K=K^*}^{K=47} \nu_{sek}$, sec^{-1}	Deexcitation rate across gap, K* to L*, R_{dex}, cm^{-3} sec^{-1}	Population of state K, N_K, cm^{-3}	Mean gap energy, E*, ev
K=47 16,1	1.85E 13	2.28E 24	1.10E 11	0.092	K=24 6,3	2.71E 12	2.47E 25	7.66E 12	0.383
12,3	9.56E 12	1.86E 24	2.76E 11	.099	10,0	3.10E 11	9.24E 23	1.14E 12	.415
14,2	5.22E 13	1.11E 25	2.15E 11	.103	8,2	7.76E 11	7.46E 24	1.14E 13	.454
15,1	9.49E 12	1.61E 24	1.32E 11	.109	9,1	5.20E 12	2.97E 25	5.56E 12	.465
11,3	5.59E 12	1.38E 24	3.41E 11	.118	9,1	4.53E 11	2.30E 24	2.96E 12	.506
13,2	2.26E 13	6.02E 24	2.72E 11	.124	5,4	1.30E 13	6.50E 26	5.10E 13	.547
14,1	6.16E 12	1.29E 24	1.69E 11	.131	5,3	8.61E 11	4.19E 25	5.40E 13	.554
10,3	3.42E 12	1.08E 24	4.50E 11	.143	9,0	1.13E 11	1.75E 24	8.41E 12	.610
12,2	1.67E 13	6.07E 24	3.73E 11	.152	7,2	2.79E 13	2.36E 27	8.46E 13	.663
13,1	3.38E 12	9.59E 23	2.33E 11	.161	7,2	3.29E 11	2.29E 25	5.81E 13	.680
9,3	1.93E 12	8.44E 23	6.53E 11	.178	8,1	1.39E 12	1.14E 26	8.40E 13	.701
11,2	9.05E 12	5.00E 24	5.74E 11	.189	8,1	8.93E 10	4.97E 24	4.73E 13	.783
12,1	1.95E 12	8.25E 23	3.64E 11	.203	4,3	1.29E 11	2.11E 26	1.96E 15	.869
12,0;8,3	1.02E 12	[a]7.50E 23	1.27E 12	.227	8,0	3.10E 10	1.36E 25	3.50E 14	.983
10,2	4.84E 12	4.88E 24	1.06E 12	.243	6,2	6.19E 12	7.31E 28	1.18E 16	1.090
11,1	3.42E 13	1.63E 25	4.56E 11	.247	6,2	4.82E 10	4.37E 26	8.38E 15	1.133
11,1	1.59E 12	8.58E 23	2.34E 11	.264	7,1	2.52E 11	5.14E 27	2.11E 16	1.184
7,3	9.58E 12	2.15E 25	2.36E 12	.281	7,1	4.57E 09	4.28E 25	1.37E 16	1.395
11,0	1.02E 12	9.55E 23	3.46E 11	.301	7,0	7.85E 09	7.20E 27	1.42E 18	1.840
9,2	2.63E 12	5.91E 24	2.66E 12	.324	5,2	9.15E 11	1.12E 33	1.22E 21	2.090
10,1	1.47E 13	1.84E 25	1.19E 12	.331	5,2	3.26E 09	2.09E 30	9.40E 20	2.267
10,1	2.17E 12	2.64E 24	6.18E 11	.356	6,1	2.09E 10	1.00E 33	5.01E 22	2.473
6,4;6,5	1.67E 13	3.40E 26	2.12E 13	.380	6,1	9.54E 07	4.64E 30	5.56E 22	3.200
					6,0			5.27E 29	

[a] $(R_{dex})_{min}$ for (12s, 8f→10d) gap; $R_{rec} = \frac{1}{3}(7.50 \times 10^{23}) = 2.50 \times 10^{23}$ cm^{-3} sec^{-1}.

TABLE III. - SUPERELASTIC COLLISION FREQUENCIES FROM ELECTRONIC STATES AND DEEXCITATION RATES ACROSS ELECTRONIC QUANTUM GAPS

[Free-electron number density, 10^{15} cm^{-3}; free-electron temperature, 5000° K.]

Electronic state (47 to 1 inclusive), K	Deexcitation frequency from state K (superelastic), $\sum_{L=1}^{L=K-1} \nu_{sek^*}$, sec^{-1}	Deexcitation rate across gap K* to L*, R_{dex}, cm^{-3} sec^{-1}	Population of state K, N_K, cm^{-3}	Electronic state (47 to 1 inclusive) K	Deexcitation frequency from state K (superelastic), $\sum_{L=1}^{L=K-1} \nu_{sek^*}$, sec^{-1}	Deexcitation rate across gap K* to L*, R_{dex}, cm^{-3} sec^{-1}	Population of state K, N_K, cm^{-3}
K=47 16,1	1.41E 13	9.26E 22	4.32E 09	K=24 6,3	3.61E 12	1.14E 23	1.99E 10
12,3	4.28E 12	7.34E 22	1.02E 10	10,0	1.51E 11	4.71E 21	2.87E 09
14,2	4.86E 13	3.98E 23	7.45E 09	8,2	1.14E 12	2.12E 22	1.65E 10
15,1	3.42E 12	6.07E 22	4.49E 09	9,1	9.23E 12	7.08E 22	6.85E 09
11,3	2.82E 12	4.97E 22	1.07E 10	9,1	2.05E 11	5.85E 21	3.47E 09
13,2	2.18E 13	1.94E 23	7.80E 09	5,4	2.60E 13	7.61E 23	2.91E 10
14,1	2.76E 12	4.31E 22	4.72E 09	5,3	9.89E 11	4.75E 22	2.94E 10
10,3	1.79E 12	3.37E 22	1.13E 10	9,0	5.88E 10	2.13E 21	4.28E 09
12,2	1.78E 13	1.64E 23	8.31E 09	7,2	6.17E 13	1.01E 24	1.63E 10
13,1	1.42E 12	2.71E 22	5.03E 09	7,2	1.20E 11	1.01E 22	1.10E 10
9,3	1.07E 12	2.16E 22	1.22E 10	8,1	2.87E 12	3.69E 22	1.18E 10
11,2	1.05E 13	1.05E 23	9.06E 09	8,1	3.53E 10	1.67E 21	6.04E 09
12,1	8.57E 11	1.81E 22	5.50E 09	4,3	2.64E 11	1.63E 22	6.03E 10
12,0;8,3	5.54E 11	1.41E 22	1.55E 10	8,0	2.00E 10	1.01E 21	9.01E 09
10,2	6.16E 12	7.01E 22	1.02E 10	6,2	1.66E 13	7.29E 23	4.39E 10
11,1	4.72E 13	2.19E 23	4.16E 09	6,2	1.77E 10	4.39E 21	2.96E 10
11,1	5.66E 11	1.26E 22	2.09E 09	7,1	6.50E 11	2.43E 22	3.56E 10
7,3	1.38E 13	2.22E 23	1.57E 10	7,1	1.25E 09	2.02E 20	1.88E 10
11,0	3.80E 11	1.10E 22	2.26E 09	7,0	1.55E 10	8,52E 20	4.75E 10
9,2	3.27E 12	4.68E 22	1.23E 10	5,2	3.03E 12	1.34E 24	4.42E 11
10,1	2.20E 13	1.31E 23	5.04E 09	5,2	7.10E 08	2.43E 21	3.03E 11
10,1	9.64E 11	1.98E 22	2.54E 09	6,1	6.95E 10	4.73E 22	6.71E 11
6,4;6,5	2.80E 13	1.59E 24	5.65E 10	6,1	7.64E 07	[a]1.32E 20	3.94E 11
				6,0			9.78E 12

[a] $(R_{dex})_{min}$ for (6p→6s) gap; $R_{rec} = \frac{1}{2}(1.32\times10^{20}\ cm^{-3}\ sec^{-1}) = 6.6\times10^{19}\ cm^{-3}\ sec^{-1}$.

NASA-Langley, 1964 E-2223